

## Article

# Numerical Approach Regarding the Effect of the Flight Shape on the Performance of Rotary Dryers from Asphalt Plants

Andrei Burlacu, Marius Gabriel Petrescu, Teodor Dumitru, Adrian Niță, Maria Tănase <sup>\*</sup>, Eugen Laudacescu, Ibrahim Ramadan and Costin Ilincă

Department of Mechanical Engineering, Petroleum Gas University of Ploiești, 100680 Ploiești, Romania

\* Correspondence: maria.tanase@upg-ploiesti.ro; Tel.: +40-726555632

**Abstract:** The distribution of aggregates in the cross-section of the drum, in the case of equipment used for the production of asphalt mixtures, essentially influences the performance of rotary dryers. In the research carried out in this article, the optimization of the distribution of particles in the active region of the drum was pursued by modifying the geometric shape of the flights, taking into account at the same time the influence of the technological parameters of operation such as drum rotation speed and drum filling degree. The studies were performed using the discrete element method (DEM), and the obtained results revealed that flight geometry strongly influences drying efficiency. The efficiency of rectangular double-angled type flights is strongly influenced by the drum rotation speed, especially at high levels of filling degree (20%), with the mass of aggregates exposed to drying increasing by 41.11% when drum rotation speed increases from 10 rpm to 15 rpm. Similarly, hook-type flights show a minimum efficiency at 15% filling degree and 15 rpm. The comparative analysis of the flight shape is not only carried out in order to establish the variant that ensures maximum drying efficiency but also from the point of view of execution technology. (Original flights can be obtained by deep drawing, but they have a complex geometric configuration; cup flights can be obtained very easily from tubular material cut on the generators; hook flights by deep drawing or welding the cut tubular material on a straight plate, and the L type by deep drawing). Taking into account that semi-finished products can be very thick, it is possible that, in some cases, hot embossing is necessary, so making them out of tubular material eliminates these inconveniences. All the presented results highlight that the rectangular, double-angled and hook-type flights are the most appropriate shapes that can be used regardless of the drum filling degree and rotation speed.



**Citation:** Burlacu, A.; Petrescu, M.G.; Dumitru, T.; Niță, A.; Tănase, M.; Laudacescu, E.; Ramadan, I.; Ilincă, C. Numerical Approach Regarding the Effect of the Flight Shape on the Performance of Rotary Dryers from Asphalt Plants. *Processes* **2022**, *10*, 2339. <https://doi.org/10.3390/pr10112339>

Academic Editors: Jamal Yagoobi and Evangelos Tsotsas

Received: 11 October 2022

Accepted: 7 November 2022

Published: 9 November 2022

**Publisher's Note:** MDPI stays neutral with regard to jurisdictional claims in published maps and institutional affiliations.



**Copyright:** © 2022 by the authors. Licensee MDPI, Basel, Switzerland. This article is an open access article distributed under the terms and conditions of the Creative Commons Attribution (CC BY) license (<https://creativecommons.org/licenses/by/4.0/>).

**Keywords:** rotary dryer; aggregates; asphalt; discrete element method; flights shape

## 1. Introduction

In order to obtain good quality asphalt, completely drying the aggregates is an important process carried out with rotary dryers containing a drum that rotates at certain speeds. The drum is slightly horizontally inclined and is equipped with flights of different shapes and sizes.

In the case of direct rotary dryers, the heat used to dry the aggregates comes from the hot gas supplied by a burner [1]. The process of drying aggregates involves significant energy consumption as well as negative effects on the environment. In order to decrease the energy consumption and the amount of toxic gas, it is necessary to increase the efficiency of drying aggregates in the drum [2] by adopting different solutions for the design of dryers. A main advantage is the generation of savings within companies in the field of asphalt mixture production, taking into account that the consumption of energy in the process of drying mineral particles is between 70–100 kWh per ton of mineral aggregates produced, resulting in approximately 22 kg of CO<sub>2</sub> [3].

Jullien [4] states that up to 97% of the energy consumed in asphalt production plants is used to dry the aggregates. Therefore, it is very important to find methods to make

the drying process more efficient. The performance of flighted rotary dryers is mainly determined by the efficiency of the contact between the particles and the hot gas [5]. The optimal drum loading and the maximum degree of use of the active area where drying occurs (obtaining a dense curtain of aggregates so that the cross-sectional area of the drum, occupied by the cascading particles, is as large as possible and remains so for as long as possible during its rotation) significantly influences the high performance of aggregate drying.

Many scientific studies [5–23] were conducted in order to evaluate the proper configuration of the flights, investigating the influence of flight type [11,12,14,17,18], flight dimensions [5,8–10,16,22,23] or the number of flights [9,10,23]. Theoretical and experimental studies have shown that a particular influence on the performance of rotary dryers is the flight configuration, which must be chosen in accordance with the characteristics of dried materials [5]. Therefore, when drying fibrous or cohesive particles, straight flights are recommended or used because the mixing speed is increased [24]. In [25], an experimental study was successfully carried out for drying filamentous particles with a straight-flight configuration for wet-cut tobacco. For free-falling materials, various other flight shapes, such as semi-circular, rectangular, angular, etc. can be used; the two-segment rectangular flights ensure the dispersion of a large number of particles in the hot gas stream.

Numerical simulations have become essential tools for studying different industrial equipment in order to optimize their design and operation. In the case of bulk solids, it is recommended to use the numerical technique based on the Discrete Element Method (DEM). This method was applied by Zhang et al. [24] to study the movement of plastic particles in the dryer equipped with straight flights, varying various parameters such as the drum rotation speed (10 rpm, 20 rpm, 30 rpm) and its filling degree (10%, 15%, and 20%), noting that an increase in drum rotation speed causes an increase in the retention ratio of the particles in the flights. When the drum rotation speed increases and its degree of filling decreases, there is an increase in the average speed and temperature of the particles. In the same way, Xie et al. [8] carried out a simulation with DEM to study the effect of the geometrical shape of two-segment straight flights, as well as the drum operating parameters (speed, degree of filling) in order to optimize the dispersion of aluminum ceramic particles. The scientific work carried out by Silveira et al. [5] is based on the analysis of the dynamics of the glass bead particles inside the rotating drum with straight flights formed by three segments, establishing optimal configurations for the geometric shapes of the flights.

Analyzing the scientific literature, it was noted that there are not many studies conducted on the influence of flight geometry on the degree of dispersion for mineral aggregate particles. The vast majority of DEM research is focused, in particular, on particles with spherical or rounded shapes due to the considerable reduction of the computation time.

The present study, based on numerical analysis with DEM, aims to establish the optimal configuration of rotary dryers for aggregates from the point of view of drying efficiency. Practically, the correlations between the geometrical shape of the flights and the working parameters, such as drum rotation speed and drum filling degree, are determined to obtain the greatest possible efficiency of the drying process, quantified by the degree of dispersion of the particles in the active area of the drum cross-section. The authors used specific techniques based on image analysis to estimate the percent of the area occupied by the particles in the active region of the drum. The performed analyses took into account the angular-sharp shape of the aggregate particle edges. In this way, the results are much closer to reality, simulating the real distribution of the particles on the active area of the drum, during the drying process. Optimum values and combinations of parameters were established and discussed, taking into account the complexity of the fabrication method for different flight configurations. Different geometrical shapes of flights offer advantages specific to the manufacturing technology. For example, the cup-type flight can be made by using a tubular semi-fabricated piece cut on two generators. This avoids cold plastic deformation or, for large thicknesses, hot plastic deformation, processes that are energy-consuming and require special equipment. The results obtained can be useful for further

practical engineering applications in the industry of asphalt mixture production, taking into account the current challenges regarding energy consumption.

## 2. Materials and Methods

The analysis was carried out for a real drying drum—ECO 2000 made by Benninghoven, with the following dimensional characteristics: inside diameter,  $D_i = 2200$  mm, wall thickness,  $t = 12$  mm, length,  $L = 8000$  mm, made of S235JR steel with 16 flights evenly distributed on its internal surface (flight length,  $L_f = 800$  mm) as can be seen in Figure 1. Due to the necessity to reduce the computation time in DEM analysis, a 1:4 scale model for the real rotary dryer and the flights were used. The geometric model was reproduced in Ansys SpaceClaim, considering for analysis and comparison, different flight shapes presented in Figure 2.



**Figure 1.** The geometrical characteristics of the real model used in the analysis: (a) flights' arrangement inside the drum, (b) the shape and dimensions of the flights.

The numerical analysis with DEM was performed with Rocky 2022 R2 software, and the particles considered in the study are crushed mineral aggregates (through mechanical methods—crushing) with complex shapes (Figure 3). In order to reduce the computational time, the maximum dimension of particles by reference to the three orthogonal directions was considered equal to 8 mm. For a more precise representation of the real model, a polyhedral geometric model with 10 corners was chosen, as seen in Figure 3b.

The density of the bulk aggregates was determined experimentally by weighing the mass of one liter of aggregates, as in Figure 4. An average value of  $1350 \text{ kg/m}^3$  was obtained for five measurements.

The contact parameters introduced in DEM simulation were chosen according to the indications from [26–28]: the static friction coefficient for stone-steel  $\mu_{s1} = 0.4$ , stone-stone  $\mu_{s2} = 0.5$ ; the dynamic friction coefficient for stone-steel  $\mu_{d1} = 0.4$ , stone-stone  $\mu_{d2} = 0.5$ ; and the restitution coefficient for stone-steel  $r_1 = 0.5$ , stone-stone  $r_2 = 0.3$ . In [26], the calibration was performed in order to verify the correctness of the parameters used in the DEM analysis, so the repose angle was determined for the same mineral aggregates as considered in the present work, using the cylinder test with slow lifting velocity. The maximum difference between DEM and experimental results for repose angle was only 5.57%.

Parametric studies were performed, corresponding to the different filling degrees of the drum (10%, 15%, and 20%) and different rotation speeds of the drum (8 rpm, 10 rpm, and 15 rpm). The specified parameters were chosen, taking into account that many studies from the scientific literature showed that drum filling degree and drum rotation speed have a great influence on the rotary dryer's functioning.

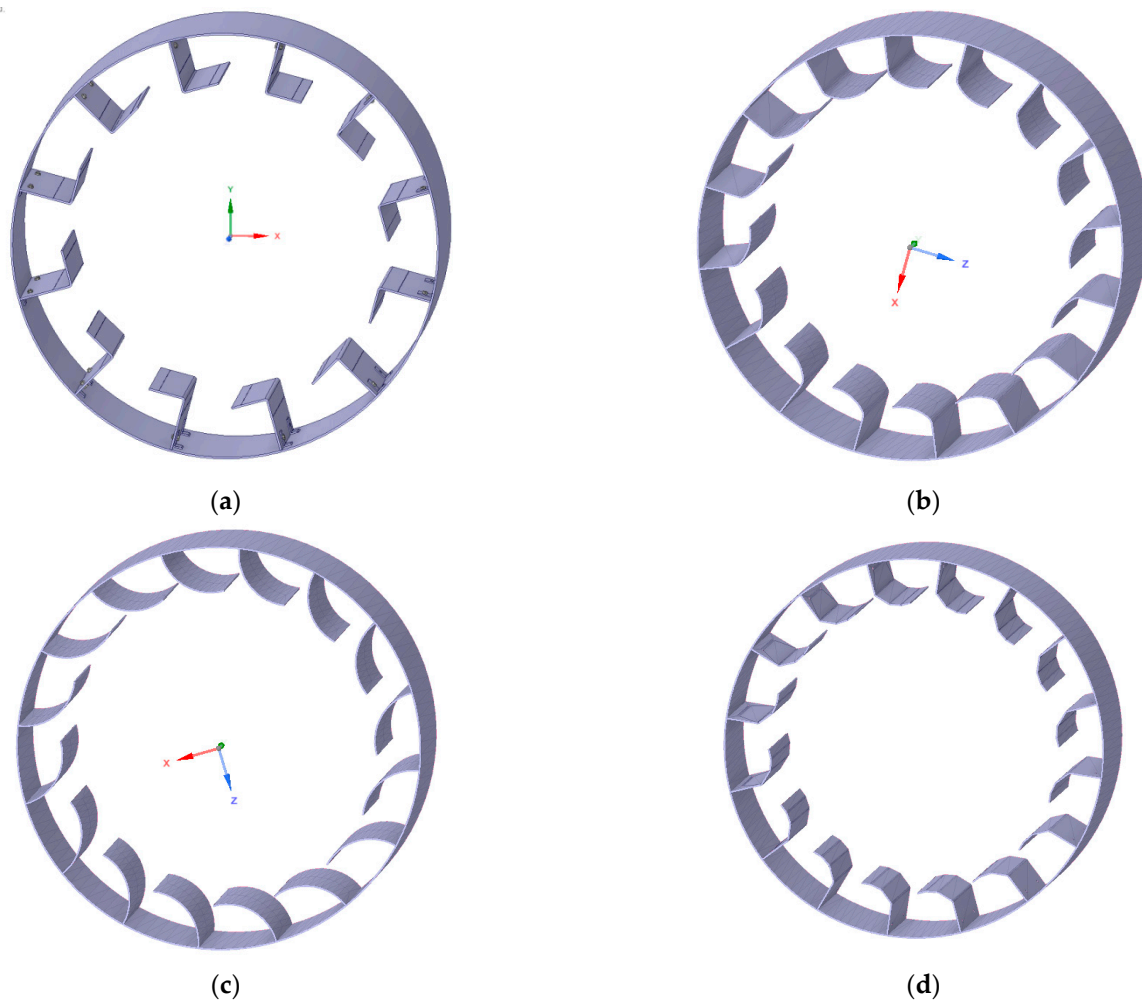
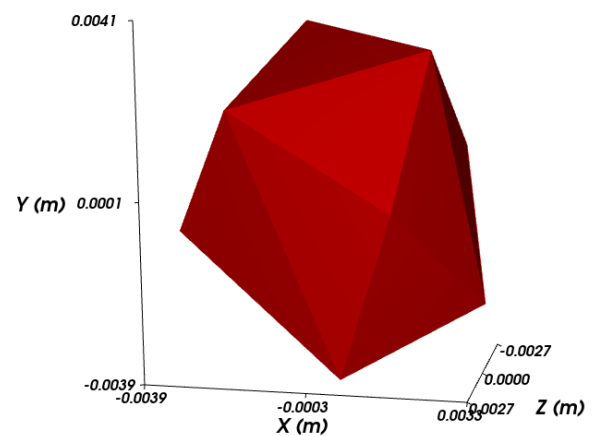


**Figure 2.** The geometrical models proposed for the analysis: (a) L-type flights, (b) hook-type flights, (c) cup-type flights, (d) rectangular double-angled type flights—the real case.



(a)



(b)

**Figure 3.** The particles used in the analysis: (a) the real shape of the aggregates, (b) the shape and dimensions of the particles used in the DEM analysis.



**Figure 4.** Determination of bulk particle density.

The above-mentioned filling degrees correspond to 4.8 kg, 7.2 kg, and 9.6 kg, respectively, of mineral aggregates. These values were determined based on the dimensional characteristics of the analyzed drum and the size and density of the stones.

The degree of dispersion of the particles in the active area of the drum was determined by calculating the percentage (*AOR*) represented by the area occupied by the particles (*AOP*), from the total active area (*TAR*):

$$AOR = \frac{AOP}{TAR} \cdot 100, [\%] \quad (1)$$

The determination of *AOR* was made with the image processing program ImageJ. In the first step, the active area of the drum was selected, then the image was converted to 8-bit grayscale (Figure 5). Therefore, the black pixels correspond to the areas occupied by particles, and the white pixels to the empty areas [5,29].

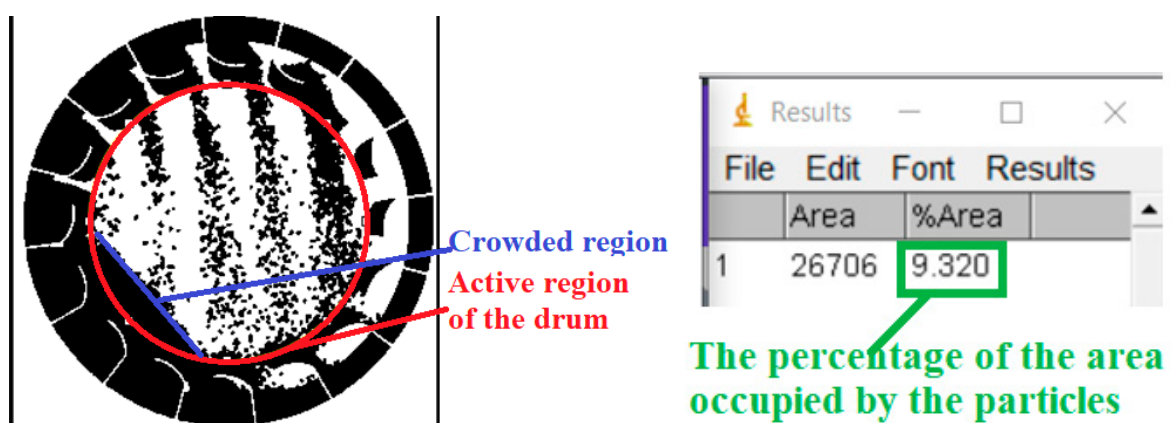


**Figure 5.** Determination of particle dispersion degree (ImageJ print screen).

For better accuracy of the obtained results, using the recommendations from [28], the area occupied by the particles (*AOP*) was calculated after excluding the crowded region (the agglomeration surfaces—Figure 5) from the bottom area of the drum.

### 3. Results and Discussion

Taking into account that the first unloading of the particles is made at 9 o'clock and the last unloading takes place at 4 o'clock, the percentages of the area occupied by the particles (*AOR*) were calculated for different positions, corresponding to 9 to 4 o'clock (with one-hour incremental steps) and the results are presented in Tables 1–4.

**Table 1.** The percentage of area occupied by the particles (*AOR* %) for L-type flights.

Position, Degree (Hour)	Filling Degree 10%			Filling Degree 15%			Filling Degree 20%		
	Rotation Speed [rpm]			Rotation Speed [rpm]			Rotation Speed [rpm]		
	8	10	15	8	10	15	8	10	15
90° (9)	0.56	0.54	0.67	0.52	0.55	0.53	0.43	0.47	0.62
120° (10)	2.59	2.32	2.29	4.40	3.75	8.45	5.63	2.57	4.83
150° (11)	9.59	10.41	19.04	16.21	17.17	25.27	18.12	19.70	27.50
180° (12)	17.69	19.95	27.56	22.62	26.68	29.39	25.21	23.56	28.54
210° (1)	20.82	27.40	22.10	22.36	26.21	23.89	22.61	27.97	31.34
240° (2)	19.17	16.47	10.46	24.41	27.22	25.02	23.91	27.88	28.20
270 (3)	12.75	13.69	9.51	21.30	19.79	17.70	21.70	29.40	26.08
300 (4)	7.62	8.77	5.82	14.06	17.00	11.31	21.83	23.33	25.26
Mean value	11.35	12.44	12.18	15.74	17.30	17.70	17.43	25.81	21.55
Average		11.99			16.91			21.60	

**Table 2.** The percentage of area occupied by the particles (*AOR* %) for hook-type flights.

Position, Degree (Hour)	Filling Degree 10%			Filling Degree 15%			Filling Degree 20%		
	Rotation Speed [rpm]			Rotation Speed [rpm]			Rotation Speed [rpm]		
	8	10	15	8	10	15	8	10	15
90° (9)	0.65	0.68	0.67	0.83	0.87	0.86	1.63	1.43	3.08
120° (10)	3.54	3.20	10.42	8.75	10.64	9.44	10.69	10.93	24.22
150° (11)	11.66	14.05	29.32	23.41	23.36	29.63	26.94	27.68	32.98
180° (12)	28.98	28.84	29.95	26.55	27.51	29.10	29.69	29.95	35.63
210° (1)	23.94	23.90	22.32	26.26	30.61	18.17	31.83	27.38	33.39
240° (2)	15.02	13.98	13.74	22.96	22.61	11.00	29.72	28.68	33.15
270 (3)	8.45	11.78	0.97	17.58	16.08	0.57	27.23	28.89	24.57
300 (4)	1.20	0.75	0.63	9.95	9.57	0.48	25.51	27.21	18.69
Mean value	11.68	12.15	13.50	17.04	17.66	12.41	22.91	22.77	25.71
Average		12.44			15.70			23.80	

**Table 3.** The percentage of the area occupied by the particles (*AOR* %) for cup-type flights.

Position, Degree (Hour)	Filling Degree 10%			Filling Degree 15%			Filling Degree 20%		
	Rotation Speed [rpm]			Rotation Speed [rpm]			Rotation Speed [rpm]		
	8	10	15	8	10	15	8	10	15
90° (9)	0.68	0.56	0.55	0.53	0.92	1.16	1.19	1.23	2.06
120° (10)	1.28	1.34	2.25	2.64	2.49	4.66	4.12	3.21	9.68
150° (11)	6.16	5.83	15.19	13.64	14.63	21.76	17.02	15.95	15.67
180° (12)	14.65	16.36	21.62	20.95	15.90	15.39	13.56	15.78	16.17
210° (1)	15.36	17.05	17.47	18.70	18.11	16.72	15.88	15.91	18.42
240° (2)	15.07	14.52	12.68	16.72	16.35	15.79	16.61	18.55	17.24
270 (3)	12.64	9.15	1.23	14.17	14.29	10.02	15.33	16.70	14.45
300 (4)	4.10	5.67	1.17	10.49	13.18	0.94	18.11	15.54	11.65
Mean value	8.74	8.10	9.02	12.23	11.98	10.81	12.73	12.86	13.17
Average		8.62			11.67			12.92	

**Table 4.** The values of the percentage of the area occupied by the particles (AOR %) for rectangular, double-angled type flights.

Position, Degree (Hour)	Filling Degree 10%			Filling Degree 15%			Filling Degree 20%		
	Rotation Speed [rpm]			Rotation Speed [rpm]			Rotation Speed [rpm]		
	8	10	15	8	10	15	8	10	15
90° (9)	1.40	1.32	1.89	2.28	3.57	3.80	2.11	3.02	4.23
120° (10)	10.11	9.83	15.65	12.65	15.10	22.83	14.29	15.48	27.65
150° (11)	17.61	17.98	28.52	22.31	25.18	30.85	33.90	21.07	34.63
180° (12)	26.34	27.98	31.36	24.66	27.40	31.72	23.86	21.82	29.55
210° (1)	20.33	21.99	16.24	23.58	26.68	31.63	22.41	20.65	30.84
240° (2)	11.49	13.37	4.20	24.91	26.24	23.54	22.43	25.18	31.56
270° (3)	5.88	6.34	0.50	21.15	20.87	17.32	22.20	24.07	33.26
300° (4)	1.94	1.47	0.60	13.22	15.54	6.35	21.75	24.98	28.80
Mean value	11.89	12.54	12.37	18.10	20.07	21.01	20.37	19.53	27.57
Average		12.26			19.72			22.49	

The results from Tables 1–4 show that the percentage of the area occupied by the particles is maintained at values above 10%:

- In the case of L-type flights, in the range 12 o'clock–3 o'clock for 10% filling degree (except for 15 rpm drum rotation speed) and 11 o'clock–4 o'clock for 15% and 20% filling degrees;
- in the case of hook-type flights, in the range 11 o'clock–2 o'clock for 10% filling degree and 11 o'clock–3 o'clock for 15% and 20% filling degrees (except for 15% filling degree and 15 rpm drum rotation speed);
- in the case of cup-type flights, in the range 12 o'clock–2 o'clock for 10% filling degree and 11 o'clock–4 o'clock for 15% and 20% filling degrees (except for 15% filling degree and 15 rpm drum rotation speed);
- in the case of rectangular, double-angled type flights, in the range 11 o'clock–2 o'clock for 10% filling degrees (except for 15 rpm) and 10 o'clock–4 o'clock for 15% and 20% filling degrees (except for 15 rpm drum rotation speed).

Similarly, as in [12], the percentage of the area occupied by the particles had an oscillatory nature during the drum rotation for all of the flight configurations, which means that the efficiency provided by a certain type of flight must be analyzed in correlation with important parameters such as drum filling degree or drum rotation speed.

For exemplification, Tables 5–7 show the particle dispersion modes for the four types of analyzed flights at 12 o'clock, corresponding to the maximum unload position.

**Table 5.** The image of the particle dispersion mode for different flights shape and 10% drum filling degree.

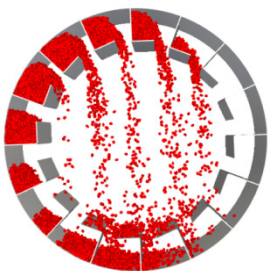
Flight Type	Drum Rotation Speed		
	8 rpm	10 rpm	15 rpm
L			

Table 5. Cont.

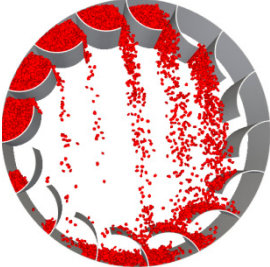
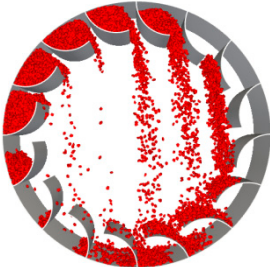
Flight Type	Drum Rotation Speed		
	8 rpm	10 rpm	15 rpm
Hook			
Cup			
Rectangular double angled			

Table 6. The image of the particle dispersion mode for different flights shape and 15% drum filling degree.

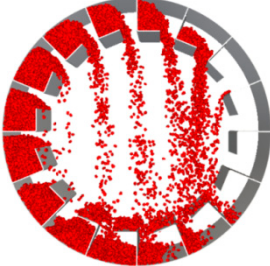
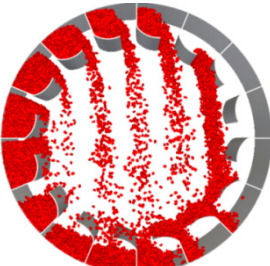
Flight Type	Drum Rotation Speed		
	8 rpm	10 rpm	15 rpm
L			
Hook			

Table 6. Cont.

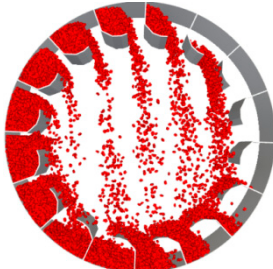
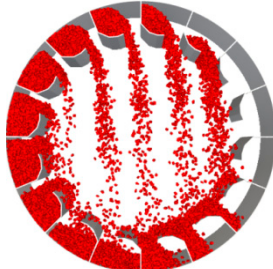
Flight Type	Drum Rotation Speed		
	8 rpm	10 rpm	15 rpm
Cup			
Rectangular double angled			

Table 7. The image of the particle dispersion mode for different flight shapes and 20% drum filling degree.

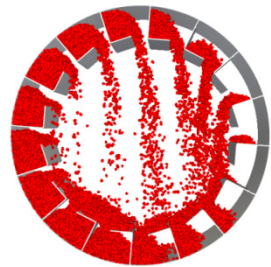
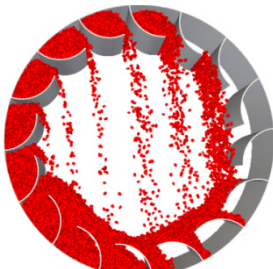
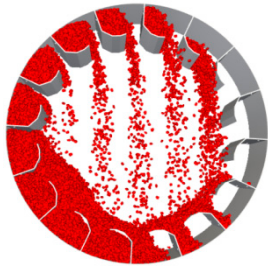
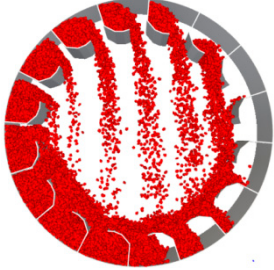
Flight Type	Drum Rotation Speed		
	8 rpm	10 rpm	15 rpm
L			
Hook			
Cup			

Table 7. Cont.

Flight Type	Drum Rotation Speed		
	8 rpm	10 rpm	15 rpm
Rectangular double-angled			

Analyzing the images presented in Tables 5–7, it can be seen that at 10% filling degree and 15 rpm, the particles are concentrated towards the lateral area of the drum, so decreasing the drying efficiency.

At 15% filling degree, there is a uniform distribution of the particles in the active area of the drum, except L-type flights.

At 20% filling degrees, in the bottom area of the drum, a crowded region appears, especially at 8 rpm, which also reduces the drying efficiency.

The results for the optimal loading of drum dryers from this paper are within the range of 10% to 15% recommended in [6] and in accordance with the optimal loading of 12.7% from reference [5].

The values of the mass of aggregates exposed to drying during a complete rotation (actually between the 9 o'clock and 4 o'clock positions) are compared in Figures 6–8, considering that the particles are uniformly distributed along the length of the drum segment.

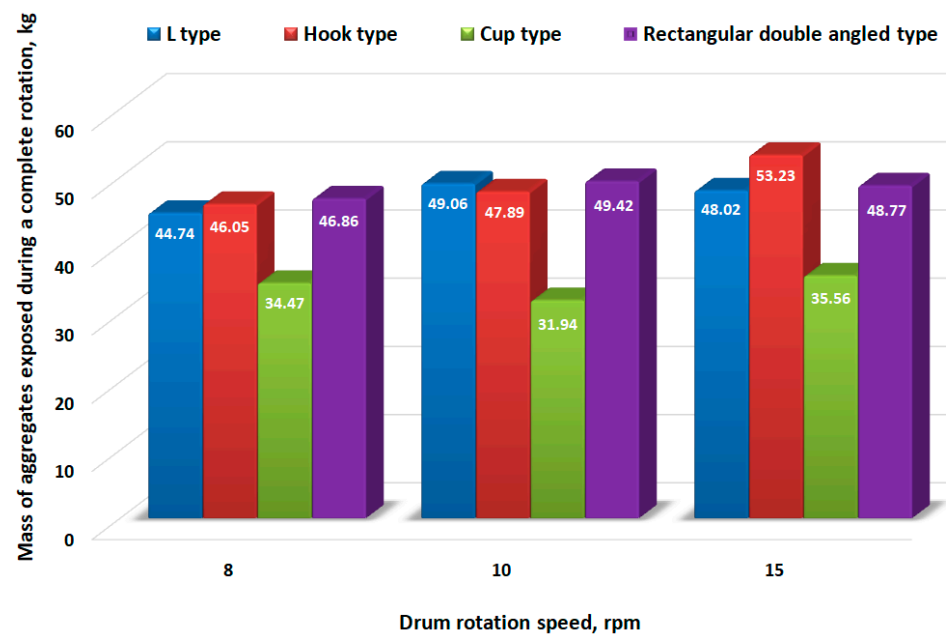


Figure 6. The influence of flight shape on the mass of aggregates exposed to drying during a complete rotation for 10% drum filling degree.

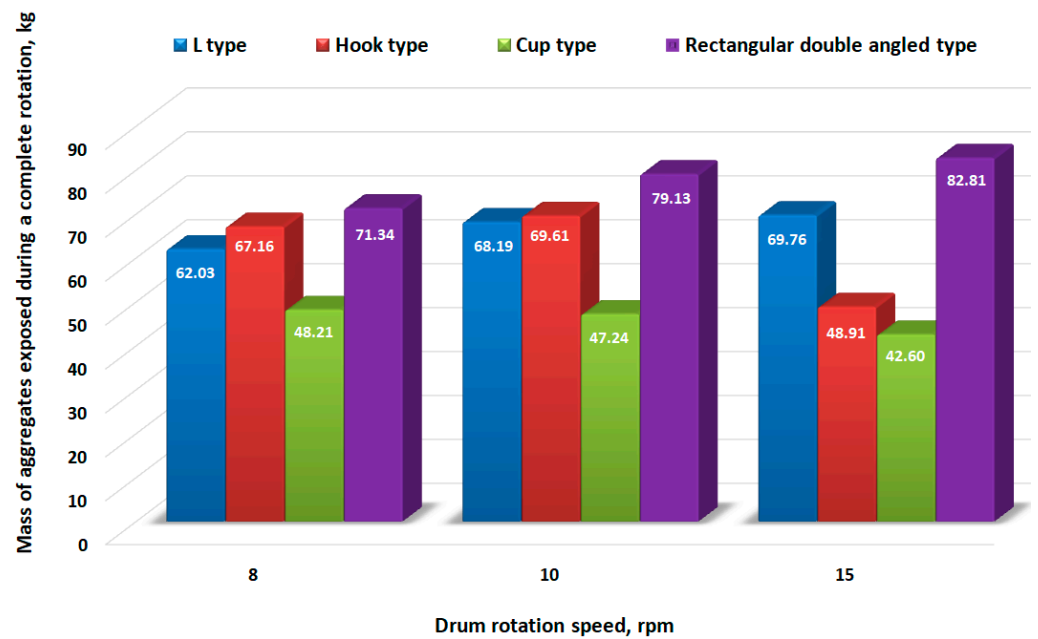


Figure 7. The influence of flight shape on the mass of aggregates exposed to drying during a complete rotation for 15% drum filling degree.

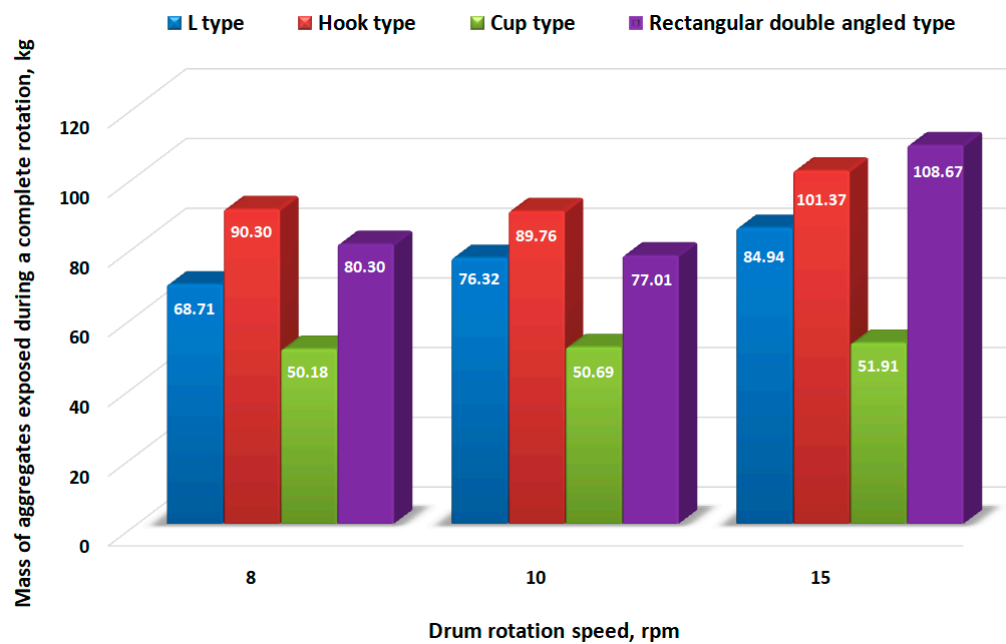


Figure 8. The influence of flight shape on the mass of aggregates exposed to drying during a complete rotation for 20% drum filling degree.

Figures 9 and 10 present a comparison between the mean values of the area occupied by the particles for different filling degrees of the drum and, respectively, for different rotation speeds for different geometrical configurations of the flights.

It can be seen that drum rotation speed does not significantly influence the mass of aggregates exposed to drying at low filling degrees (10%). Thus, an increase of 11.15% in the mass of aggregates exposed to drying when the drum rotation speed increased from 10 rpm to 15 rpm was observed for hook-type flights.

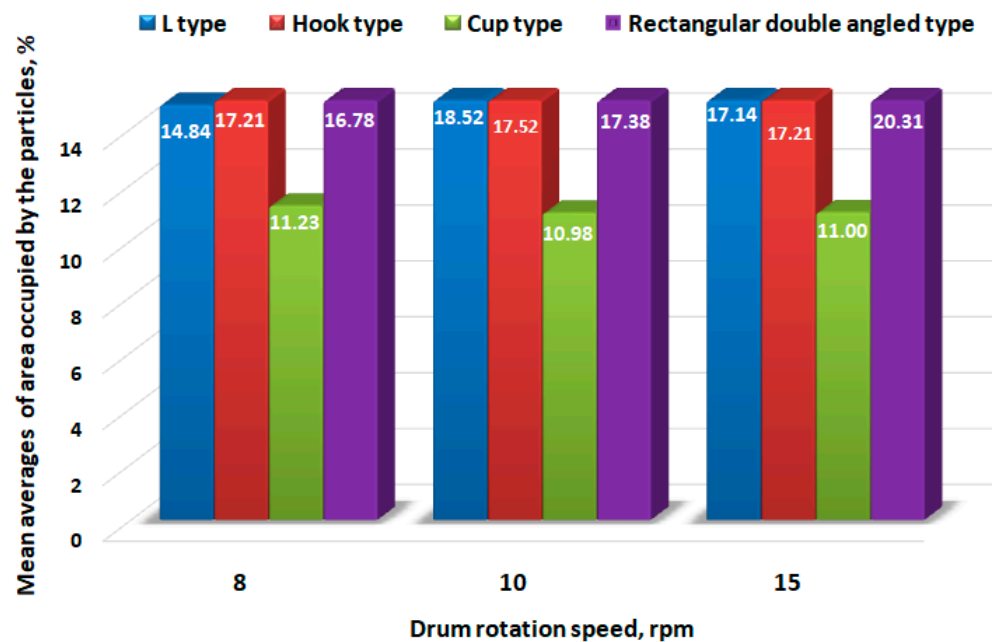


Figure 9. The influence of flight shape on the dispersion degree of the particle for different drum rotation speeds.

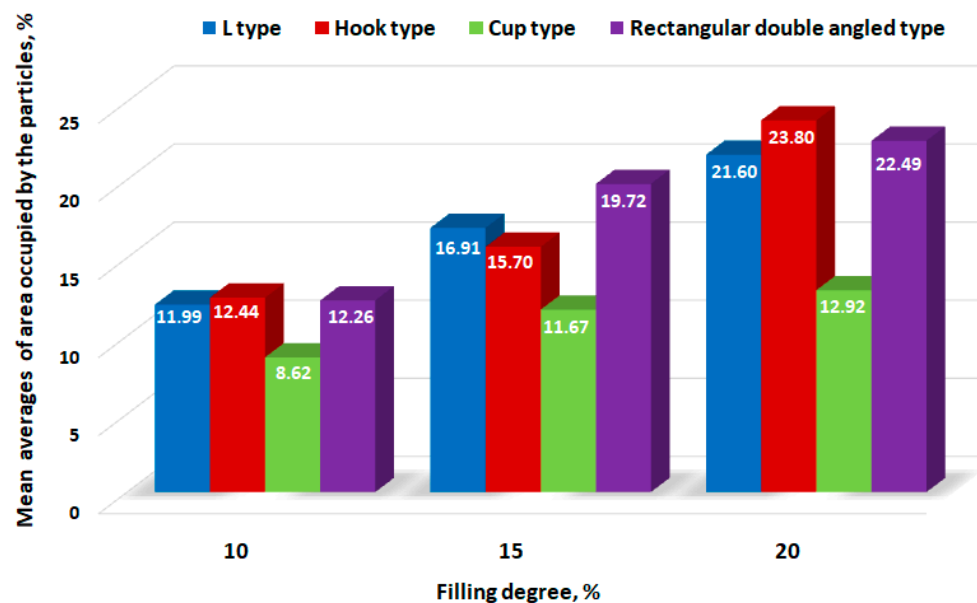


Figure 10. The influence of flight shape on the dispersion degree of the particle for different drum filling degrees.

For hook-type flights, at 15% filling degree, when the drum rotation speed increases from 10 rpm to 15 rpm, the mass of aggregates exposed to drying decreases by 42.32%.

At 20% filling degrees, there is a significant increase (41.11%) in the mass of aggregates exposed to drying in the case of rectangular, double-angled type flights.

Therefore, it can be concluded that at low filling degrees (10%), the influence of the drum rotation speed on the drying efficiency is not significant. However, for higher values of filling degree (15% and 20%), it is necessary to take into account the drum rotation speed, the rectangular double-angled type flights having maximum efficiency at 15 rpm. In comparison, in the case of hook-type flights, the minimum value of the mass of aggregates exposed to drying is obtained at 15% filling degree and 15 rpm.

Similarly, the numerical study conducted in [8] has shown that drum rotation speed has an important role in the particle distribution in the active area of the drum. It was found that in the case of straight flights and 15% drum filling degree, when the rotation speed of the drum increases from 25 rpm to 35 rpm, the percentage of the area occupied by the particles and the mass of aggregates exposed to drying increase. In contrast, for 40 rpm drum rotation speed, the values of these parameters decrease due to the centrifugal force that plays the dominant role in the motion of the particles.

Analyzing the results presented in Figures 6–10, the following conclusions can be highlighted:

- The cup-type flights have the lowest efficiency, justified by the high degree of particle retention during rotation;
- L-shaped flights generally have satisfactory performance, comparable to double-angled rectangular flights at low filling degrees (10%) and noticeably lower at 15% and 20% filling degrees, with one exception—at 20% filling degree and 10 rpm rotation speed where the efficiency is similar;
- Hook-type flights have similar performances to rectangular double-angled flights, the differences depending on the filling degree. Thus, at 10% filling degree, the results are similar; at 15% filling degree, rectangular double-angled flights have a higher efficiency; at 20% filling degree, the hook-type flights have a higher efficiency, being slightly exceeded only at 15 rpm rotation speed;

Regardless of the filling degree, the hook-type flights show a stable efficiency at rotation speeds of 8 rpm and 10 rpm. Rectangular double-angled flights show a clearly superior performance at high rotation speed (20 rpm).

The filling degree required for optimal loading is strongly influenced by the flight geometry rather than by the operating parameters such as drum rotation speed, so, based on the results obtained, the conclusions of the papers [30,31] are confirmed.

#### 4. Conclusions

The present study focused on the numerical analysis using DEM in order to highlight the influence of flight shape on the efficiency of the drying degree for mineral aggregates, assessed by determining the area occupied by the dispersed particles in the active zone of the rotary dryer drum.

Generally, the particles unloading from the flights start when the flight tip is at the 9 o'clock position and it ends around the 4 o'clock position.

Analyzing the obtained values, it was found that, regardless of the flight shape, the maximum efficiency is obtained for the drum rotation speed of 15 rpm, respectively 20% filling degree.

Using the vast amount of obtained data, it was shown that the flight shape significantly influences the degree of dispersion of the particles inside the drum.

The flight shape has an important role in the retention time of the particles on the peripheral area of the drum and, therefore, must be correlated with the rotation speed to identify the optimal solution regarding the particle dispersion. The flight shape should be chosen, also taking into account the drum filling degree, for the same reasons regarding the retention of particles on the flights.

In order to obtain high stability of the values representing the volume of the aggregate exposed to drying during a complete rotation of the drum for a wide range of filling degrees and rotation speeds, the most proper are the hook-type flights. At the same time, the efficiency is high, similar to rectangular double-angled flights.

Even though the rectangular double-angled flights show, on average, the best performance in terms of particle exposure to drying, their performance still presents a wide range in relation to the technological parameters: rotation speed and filling degree.

Compared to other similar research, we have introduced close-to-reality configurations for the aggregate materials that are subjected to drying. In most studies in the scientific literature, the particles are assimilated to spheres and refer, in particular, to cereal seeds,

glass, or steel balls. In the present paper, the mineral particles obtained by crushing the stones were studied. The particles have a complex polyhedral shape that certainly affects the constructive integrity of the equipment; this problem will be the subject of a future scientific paper. This complex shape of the particles requires very large computing resources in DEM analysis.

By comparison with the results of other researchers, the trajectories described by the particles are similar (something that confirms the correctness and quality of the model), being dependent in particular on the mass of the particles and the kinematic parameters of the equipment (especially the drum rotation speed). Some differences in the degree of dispersion of the dried particles are generated by the interaction mechanism between the aggregate particles (particle–particle) and between the particles and the flights of the drum, the contacts being linear or on a surface, unlike the sphere model (practiced by most researchers) where the contacts are point-like.

**Author Contributions:** Conceptualization, A.B., T.D. and A.N.; methodology, M.G.P.; software, C.I. and M.T.; validation, E.L. and M.T.; formal analysis, M.G.P.; investigation, M.T. and E.L.; resources, A.B.; data curation, M.T.; writing—original draft preparation, M.T., I.R. and E.L.; writing—review and editing, M.T.; visualization, C.I.; supervision, M.G.P.; project administration, M.G.P.; funding acquisition, A.B., A.N. and T.D. All authors have read and agreed to the published version of the manuscript.

**Funding:** This research received no external funding.

**Informed Consent Statement:** Not applicable.

**Conflicts of Interest:** The authors declare no conflict of interest.

## References

1. Le Guen, L.; Huchet, F.; Tamagny, P. Drying and Heating Modelling of Granular Flow: Application to the Mix-Asphalt Processes. *J. Appl. Fluid Mech.* **2011**, *4*, 71–80.
2. Wen, H.; Zhang, K. Simulation of Aggregates Heating in Asphalt Plants. *J. Eng. Mech.* **2014**, *239*, 19–28.
3. Cimbola, Z.; Dolacek-Alduk, Z. Managing Thermal Energy of Exhaust Gases in the Production of Asphalt Mixtures. *Tech. Gaz.* **2018**, *25* (Suppl. S2), 444–451.
4. Agnès, J.; Gaudefroy, V.; Ventura, A.; de la Roche, C. Airborne Emissions Assessment of Hot Asphalt Mixing. *Road Mater. Pavement Des.* **2010**, *11*, 149–169.
5. Silveira, J.; Lima, R.; Brandao, R.; Duarte, C.; Barrozo, M. A Study of the design and arrangement of flights in a rotary drum. *Powder Technol.* **2022**, *395*, 195–206. [[CrossRef](#)]
6. Lisboa, M.H.; Vitorino, D.S.; Delaiba, W.B.; Finzer, J.; Barrozo, M.A. Study of particle motion in rotary dryer. *Braz. Chem. Eng.* **2007**, *24*, 365–374. [[CrossRef](#)]
7. Revol, D.; Briens, C.L.; Chabagno, J.M. The design of flights in rotary dryers. *Powder Technol.* **2001**, *121*, 230–238. [[CrossRef](#)]
8. Xie, L.; Yang, L.; Su, L.; Xu, S.; Zhang, W.A. Novel Rotary Dryer Filled with Alumina Ceramic Beads for the Treatment of Industrial Wastewaters: Numerical Simulation and Experimental Study. *Processes* **2021**, *9*, 862. [[CrossRef](#)]
9. Seidenbecher, J.; Herz, F.; Meitzner, C.; Specht, E.; Wirtz, S.; Scherer, V.; Liu, X. Experimental analysis of the flight design effect on the temperature distribution in rotary kilns. *Chem. Eng. Sci.* **2021**, *240*, 116652. [[CrossRef](#)]
10. Sunkara, K.R.; Herz, F.; Specht, E.; Mellmann, J.; Erpelding, R. Modeling the discharge characteristics of rectangular flights in a flighted rotary drum. *Powder Technol.* **2013**, *234*, 107–116. [[CrossRef](#)]
11. Portnikov, D.; Ziskind, Z.; Kalman, H. Experimental and computational study of a flighted rotary drum cross-sectional characteristics. *Powder Technol.* **2022**, *403*, 17398. [[CrossRef](#)]
12. Silveira, J.C.; Brandao, R.J.; Lima, M.R.; Machado, M.V.C.; Barrozo, M.A.S.; Duarte, C.R. A fluid dynamic study of the active phase behavior in a rotary drum with flights of two and three segments. *Powder Technol.* **2020**, *368*, 297–307. [[CrossRef](#)]
13. Ghasemi, A.; Hasankhoei, A.; Parsapour, G.; Razi, E.; Banisi, S. A combined physical and DEM modelling approach to improve performance of rotary dryers by modifying flights design. *Dry Technol.* **2020**, *39*, 548–565. [[CrossRef](#)]
14. Li, H. Numerical simulation of the dryer drum radiation area using coupled CFD and DE Methods. *IOP Conf. Ser. Earth Environ. Sci.* **2021**, *618*, 012047.
15. Sunkara, K.R.; Herz, F.; Specht, E.; Mellmann, J. Influence of flight design on the particle distribution of a flighted rotating drum. *Chem. Eng. Sci.* **2013**, *90*, 101–109. [[CrossRef](#)]
16. Karali, M.A. Analysis Study of the Axial Transport and Heat Transfer of a Flighted Rotary Drum Operated at Optimum Loading. Ph.D. Thesis, Otto-von-Guericke University Magdeburg, Magdeburg, Germany, 2015.

17. Benhsine, I.; Hellou, M.; Lominé, F.; Roques, Y. Influence of flight shape on discharging profiles of granular material in rotary dryer. *Eur. Phys. J. Conf.* **2017**, *140*, 03023. [[CrossRef](#)]
18. Savalagi, P.; Chittappa, H.C. Flight design for rotary bagasse dryer. *Int. Res. J. Eng. Technol.* **2017**, *4*, 920–925.
19. Ajayi, O.O.; Sheehan, M.E. Design loading of free flowing and cohesive solids in flighted rotary dryers. *Chem. Eng. Sci.* **2012**, *73*, 400–411. [[CrossRef](#)]
20. Van-Puyvelde, D.R. Modelling the hold up of lifters in rotary dryers. *Chem. Eng. Res. Des.* **2009**, *87*, 226–232. [[CrossRef](#)]
21. Lee, A.; Sheehan, M.E. Development of a geometric flight unloading model for flighted rotary dryers. *Powder Technol.* **2010**, *198*, 395–403. [[CrossRef](#)]
22. Karali, M.A.; Herz, F.; Specht, E.; Mallmann, J. Comparison of image analysis methods to determine the optimum loading of flighted rotary drums. *Powder Technol.* **2016**, *291*, 147–153. [[CrossRef](#)]
23. Xie, Q.; Chen, Z.; Mao, Y.; Chen, G.; Shen, W. Case studies of heat conduction in rotary drums with L-shaped lifters via DEM. *Case Stud. Therm. Eng.* **2018**, *11*, 145–152. [[CrossRef](#)]
24. Zhang, L.; Jiang, Z.; Weigler, F.; Herz, F.; Mellmann, J.; Tsotsas, E. PTV measurement and DEM simulation of the particle motion in a flighted rotating drum. *Powder Technol.* **2020**, *363*, 23–37. [[CrossRef](#)]
25. Gu, C.; Li, P.; Yuan, Z.; Yan, Y.; Luo, D.; Li, B.; Lu, D. A new corrected formula to predict mean residence time of flexible filamentous particles in rotary dryers. *Powder Technol.* **2016**, *303*, 168–175. [[CrossRef](#)]
26. Niță, A.; Laudacescu, E.; Ramadan, I.; Petrescu, M.G. An Example for Determining the Physical Parameters Used in DEM Modeling for the Interaction Process between Aggregates and Working Equipment. In Proceedings of the 10th International Conference on Advanced Concepts in Mechanical Engineering—ACME 2022, Iasi City, Romania, 9–10 June 2022.
27. Dumitru, T.; Ilincă, C.; Tănase, M. Influence of technological parameters on the behaviour in operation of the asphalt milling equipment. In Proceedings of the 10th International Conference on Advanced Concepts in Mechanical Engineering—ACME 2022, Iasi City, Romania, 9–10 June 2022.
28. Burlacu, A.I.; Tănase, M.; Ilincă, C.; Petrescu, M.G. Optimizing the trajectory of aggregates in drying units from the asphaltplants. In Proceedings of the 10th International Conference on Advanced Concepts in Mechanical Engineering—ACME 2022, Iasi City, Romania, 9–10 June 2022.
29. Ajayi, O.O.; Sheehan, M.E. Application of image analysis to determine design loading in flighted rotary dryers. *Powder Technol.* **2012**, *223*, 123–130. [[CrossRef](#)]
30. Karali, M.; Sunkara, K.R.; Herz, F.; Specht, E. Experimental analysis of a flighted rotary drum to assess the optimum loading. *Chem. Eng. Sci.* **2015**, *138*, 772–779. [[CrossRef](#)]
31. Karali, M.; Specht, E.; Herz, F.; Mellmann, J.; Refaey, H. Unloading characteristics of flights in a flighted rotary drum operated at optimum loading. *Powder Technol.* **2018**, *333*, 347–352. [[CrossRef](#)]